IEEE Access
Multidisciplinary : Rapid Review : Open Access Journal

Received June 27, 2017, accepted August 18, 2017, date of publication September 1, 2017, date of current version November 14, 2017.

Digital Object Identifier 10.1109/ACCESS.2017.2748360

Ground Motion Prediction Equations for Malaysia Due to Subduction Zone Earthquakes in Sumatran Region

M. S. LIEW[1], KAMALUDDEEN USMAN DANYARO[1], MAZLINA MOHAMAD[1], LIM EU SHAWN[1], AND AZIZ AULOV[2]
[1]Universiti Teknologi PETRONAS, Seri Iskandar 32610, Malaysia
[2]Airport Consulting Partners GmbH Beratende Ingenieure, 70197 Stuttgart, Germany

Corresponding author: Kamaluddeen Usman Danyaro (kamaluddeen.usman@utp.edu.my)

This work was supported by Universiti Teknologi PETRONAS, Seri Iskandar 32610, Malaysia.

ABSTRACT There has been numerous seismic hazard studies so far that includes Malaysian territories. However, there is a need to assess how reliable those studies are. Two main potential contributors to error have been identified: 1) seismic hazard analysis method and 2) ground motion prediction equation (GMPE). The amount of variation in predicting erroneous GMPE is huge. Thus, this paper concentrates on generating new GMPEs due to subduction specified for Malaysia and validated against developed GMPE. Empirical method for GMPE generation was utilized using recorded ground motion data acquired from the Malaysian Meteorological Department. The earthquakes were grouped according to the source, and only source types in the Sumatran subduction area were used due to the availability of enough data to identify a pattern. Three GMPEs were generated for three different source types, namely, shallow subduction earthquake, deep subduction earthquake, and backarc earthquake sources. Sumatran strike slip fault is considered within backarc seismicity. They were compared with the models proposed by Petersen (modified from Young), Atkinson and Boore, and Megawati. The comparison results showed that the proposed models are far superior at predicting the earthquakes in the Sumatran region, with percentage difference between estimates and the recorded values being the lowest. Therefore, the equations should be used in further seismic hazard analyses. Thus, this paper becomes a part of the recent initiatives in Malaysia to assess the hazards posed by earthquakes.

INDEX TERMS Ground motion prediction equation, earthquakes in Malaysia, earthquakes in the sumatran region, seismic hazard.

I. INTRODUCTION

Malaysia has seen a remarkable boom in industrialization in the past century in almost all sectors of economy; the oil and gas sector being no exception. The oil and gas sector plays a vital role in the Malaysian economy due to its significant contribution to workforce and government activities, as well as to its share of energy provisions. The statistics are staggering: 86.4% of energy consumed in Malaysia was generated from oil and gas in 2010 [1], transport and industrial sectors being main consumers, each constituting 40.5% and 38.6% of energy use respectively. Considering estimates by the International Energy Agency, where 70% growth in energy demand is anticipated in the next 17 years [2], growth in oil and gas demand is expected to increase sharply in the coming years.

Malaysia has three main oil producing basins: the Malay basin, which is located to the west of offshore Peninsular Malaysia (PMO), the Sabah (SBO) and Sarawak (SKO) basins [3], [4]. Most oil reserves are located in the Malay basin, and the oil itself is mostly of high value due to its quality, while gas reserves are concentrated in offshore Sabah basin. To extract these hydrocarbon resources, a large number of platforms were utilized in the oil and gas exploration and production activities since early 1960s. Fixed structures in the Malaysian South China Sea (MSCS) are installed in waters of up to 140m depth. Offshore fixed platforms in these waters range from 15m to 150m height, the tallest of which will roughly equal to a 50-storey high-rise building onshore with natural periods of around 5 seconds, therefore being vulnerable to long period waves generated by distant earthquakes [4]. Shorter platforms will also be affected by earthquakes, but the earthquakes will have to occur close to platform locations to amplify with their long natural periods.

The platforms in MSCS have been designed to withstand environmental loads anticipated in the region as per PETRONAS Technical Standards (PTS) and American Petroleum Institute (API) code requirements. PTS code (34.19.10.30) specifies that earthquake loading has to be done according to API code (RP-2A-WSD-2000). API code states that for the zones of low seismic activity, where ground acceleration is less than 0.05g, no earthquake analysis is required, as it is assumed that the design for environmental loadings will provide sufficient resistance against potential effects from earthquakes. The PTS code is conservative with respect to the environmental criteria chosen, which have been formulated for North Sea conditions that are way harsher than MSCS conditions [5]. Thus, adequate ‘‘safety cushion’’ is provided against seismic effects of the low seismicity zone.

A. EARTHQUAKES IN THE MALAYSIAN CONTEXT

There have been numerous earthquakes in the region that caused tremors on Malaysian soil, such as the regionally devastating instances of 2004 Aceh (M_w of 9.1) and 2005 Nias (M_w of 8.6) earthquakes. As in March 2012, ground shake due to raptures in the Indian Ocean (M_w of 8.2) on the Australian Plate was clearly felt, causing a short panic among residents of cities throughout Malaysia [6], [7]. Given such regular occurrences of ground shake great enough to sway high-rise buildings, there was a well-founded worry if MSCS and Malaysia as a whole are really within a low-seismic zone with ground accelerations below 0.05g. The Construction Industry Development Board of Malaysia (CIDB) was quick to mobilize researchers and academicians to help analyse the earthquake threat. Nevertheless, debates among the construction and engineering professionals still persist on the practicality of imposing seismic considerations.

Now, due to recent big earthquakes, there was a sudden need for a Seismic Hazard Analysis (SHA) for Malaysia that would help designers choose appropriate design considerations. There have been numerous SHAs conducted in the region, several of which did include MSCS in their study window [8]–[15]. However, Petersen *et al.* [14] have produced a seismic hazard map for South East Asia that includes onshore and offshore Malaysian areas within their studies.

However, the results of these published works are not applied in industry as desired. A thorough study of the methodology has shown that these studies have a component that is highly disputable and subjective, and affects the study results in a profound manner, namely ground motion prediction equation (GMPE) [16]. GMPE is an equation used to calculate the level of ground shake at a desired distance from the earthquake epicenter. All of the GMPEs used for regional SHA are ‘‘imported’’ equations that have been developed mainly for the Americas. Certainly, lying on the stable portion of the Sunda plate, Malaysia is influenced by interplate and subduction zone ruptures, which makes it a completely different scenario than what the ‘‘imported’’ equations were developed from and for [17]. This indicates that there is a crucial need for a fully-verified, Malaysia-specific equation that will be used in SHAs conducted for Malaysia in the future. Therefore, the objective of this paper is to establish a framework for seismic source classification and perform grouping of earthquakes according to their sources. It will be followed by development, comparison and verification of Malaysia-specific GMPEs for all earthquake sources against recorded data and available GMPEs in the literature.

II. RELATED WORKS

Earthquake is a very frequently occurring phenomenon throughout the world that on average, every 20 minutes an earthquake is recorded by the network of NEIC [22]. In view of such a staggering activity, it is useful to first understand how earthquakes are generated and propagated particularly in the Malaysian scenario and Sumatran region.

There are four types of earthquake regions which are also known as seismic regions [23]:

i. Midocean ridges – Seismic activity is low and very shallow, mainly because of thin crust and little stress build-up due to divergence.
ii. Transform zones- Seismic activity is of considerable size, as two plates scraping along can lead to significant stress build-up.
iii. Subduction zones – Two plates collide, whereas one plate overrides the other creating immense stress build-ups. In such regions, one can see deep trenches and mountain regions located along each other.
iv. Boundary zones – Boundaries around continental plates have moderate seismicity, caused by stress released from mountain ranges.

It is worth noting that there are earthquakes occurring within the interiors of continental plates, but it is just that their nature is highly unpredictable and their intensity is moderate at best. The earthquakes usually occur at faults spread out throughout the plates, and detecting these faults is rather difficult: the productive faults are mapped easily, while those faults whose stress build-up period is longer than the recorded history are not as easily mapped. These are almost impossible to predict, unless some activity is recorded.

A. SEISMIC PROPAGATION

Seismic event is a sudden release of energy which will then be dispersed to surroundings in all direction. With the release of energy, the energy propagates outward in the form of seismic waves [24]. These are categorised as surface waves and body waves. Surface waves cause the most damage and are trapped in the outer layer of the earth's crust [25]. There are two types of surface waves: Love waves (side-to-side) and Rayleigh waves (rolling) [26]. Love waves are faster than Rayleigh waves.

Body waves are faster than surface waves and can travel through the Earth media. There are two types of body waves:

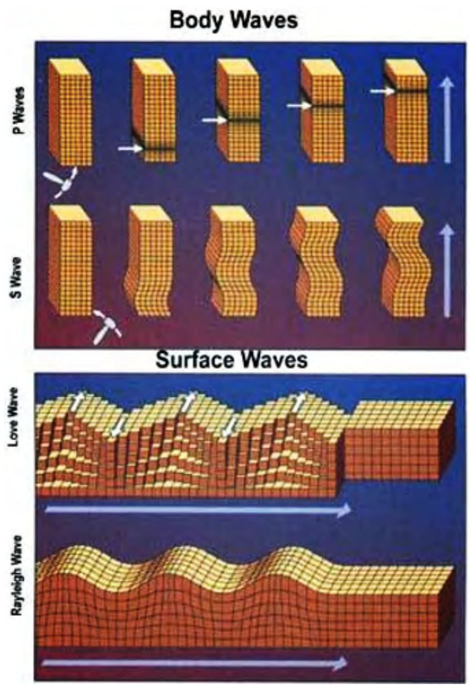

FIGURE 1. Web propagation types and particle displacement mechanisms [22].

P-waves (compressional) and S-waves (shear). P-Waves are faster than S-waves, thus they are recorded first by the seismograph. In addition, P-waves cause more damage than S-waves, because they temporarily change the area and the volume of the ground, damaging many of the human-made structures that are situated on that ground. Fig. 1 shows all waves and their ground displacement characteristics.

Out of high and low frequency waves, only the low frequency, long period waves are able to reach far-fields due to their robustness in preserving energy, unlike the high frequency short period waves, that lose much of their energy very fast and get damped out in a shorter distance [27].

The body waves that travel through rock layers for very large distances arrive at the site, and transfer the energy to the soil layer above. Depending on the soil type, this transfer can either amplify [28] or dampen the seismic energy. The Mexico City earthquake of 1985 showed how small amounts of energy can lead to high damage due to soil amplification alone. Even though soil layers in Malaysian cities do not amplify the waves to that extent, there is an indication that amplification does exist [29]. In fact, Marto et al. [30] have calculated an amplification factor of nearly 2.5 at 2% chance of exceedance in 50 years for Kuala Lumpur City Center in their micro-zonation map.

B. RECORDING AND SCALES

Historically, there was a need for some form of measurement of earthquakes. Though simplifying such a complex event is no mean feat, scientists have developed several magnitude scales that cater to specific purposes [31].

One of the most important parameters characterizing an earthquake is its "size". It has been measured to be directly related to the energy released. However, Richter [32] initially used local magnitude scale (M_L), which was defined using trace amplitudes of local earthquakes recorded on typical Wood-Anderson seismographs ($T_0 = 0.8$s, critical damping 0.8, V = 2, 800). Notably, the earthquake magnitude is the most common measure of the size of an earthquake. Also, the termed M_L, the scale was widely used throughout the first three quarters of the 20th century [33]. Unfortunately, due to instrument limitations and measurement of a single, short-period peak height, the scale saturates and fails to accurately convey the amount of energy released by earthquakes greater than M_L 6.5 [34]. Another limitation of this scale is that the measurement has to be done within 100 km to the epicenter. Despite this, M_L continues to be a popular tool for computing the relative size of earthquakes.

In order to solve saturation problems in M_L, Surface-Wave Magnitude (M_S) was developed. M_S is a measurement scale that is based on the Rayleigh surface waves [35] that have periods of around 20 seconds [36]. Also, not being bound by any distance for measurement, this scale has been used for empirical comparisons of magnitude versus earthquake rupture lengths. However, the shortcoming of this particular scale is that it also saturates at magnitudes greater than M_S 8 [33].

The development of scale continues with Body-Wave Magnitude (mb). mb is another scale developed by Richter and Gutenberg that is based on P-wave records [35], with periods of around 10 seconds [36], with the purpose of treating deep earthquakes [31]. It is a widely reported magnitude by modern-day stations, even though its saturation point is around mb 8 [33]. Unfortunately, the saturation problem persists. When the peak of the energy spectrum lies below the frequency range of the Wood-Anderson seismograph, the seismograph fails to accurately predict the magnitude resulting in what is known as "saturation" [31]. This has led to the development of a new scale known as Moment Magnitude (M_w or M). It is a popular scale [37] proposed by Kanamori [38] and later refined by [34] and [39] that is rather different in its approach to quantify earthquake energy.

The Seismic moment (M_0) of the earthquake serves as the basis of this scale, and is utilized to directly represent the amount of energy released at the source. Equation (1) shows the formula used to compute M_0 [36]:

$$M_0 = D \times A \times \mu \tag{1}$$

where

- D average displacement over entire fault surface
- A area of the fault surface
- μ average shear rigidity

Fundamentally, this means that Moment Magnitude tries to directly quantify the energy released by the earthquake, rather than to try to calculate it from earthquake effects on individual stations [31]. This way, M_w succeeds at overcoming the saturation problems of other scales and is the most reliable among them [35]. Equation (2) shows the formula used to compute M_w [39]:

$$M_w = 2/3 \times \log M_0 - 10.7 \qquad (2)$$

1) THE MALAYSIAN SCENARIO

Malaysia is located in a stable region of the Southeast extension of the Eurasian plate, known as Sunda plate, surrounded by active interplate boundaries, such as the boundaries between the Eurasian and Philippines Sea Plates in the East and between Indo-Australian and Eurasian plates to the West [8]. Therefore, because of its location, tremors experienced in Malaysia are mainly due to the neighbouring Sumatran subduction zone and the Sumatran fault. Fig. 2 shows the distribution of earthquakes in the region [9]. Zone 1 is the Sumatran Subduction Zone, while Zones 2 and 3 denote the Sumatran Fault.

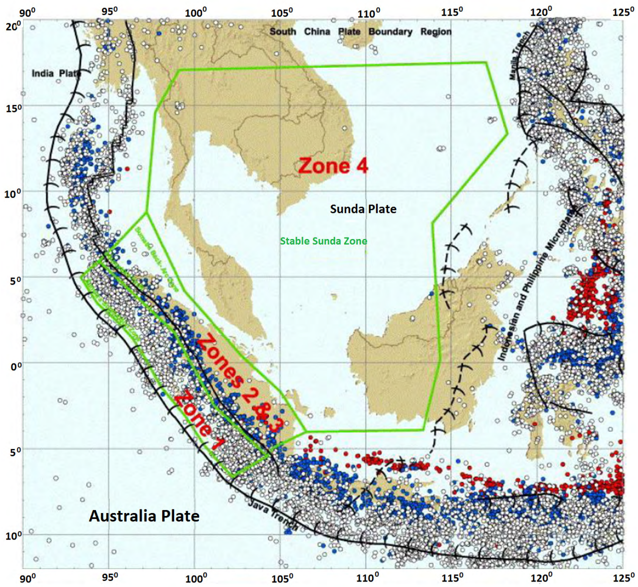

FIGURE 2. Distribution of earthquake epicenters in South East Asia [14].

The Sumatran fault is more than 1500km long and runs through entire Sumatra. Being a strike slip fault, it stores the energy through shear deformation of the rocks when the edges on both sides of the plate get interlocked [40]. In such a setting, it is widely accepted that not much energy could be stored. Hence, earthquakes with extra-large magnitudes are not expected here. Historical records for the Sumatran strike slip fault show that the biggest earthquakes occurred in 1892 (M_w 7.7) and in 1943 (M_w 7.6).

The Sumatran Subduction Zone is a result of the subduction of Indian-Australian plate beneath the Eurasian plate and is located some 600 km away from Malaysia in its nearest neighbours. The rate of subduction is about 67 mm per year [41]. The subducted slab moves at a shallow angle and the overriding and subducting plates are strongly coupled, giving way for strong earthquakes. This source is able to generate earthquakes of great sizes [27]. Historical records for the last 300 years show four major earthquakes occurring in this zone. First two earthquakes occurred in 1833 (M_w 8.75) and in 1861 (M_w 8.4), while the other two occurred recently: the Aceh earthquake in December 2004 (M_w 9.1) and the Nias earthquake in March 2005 (M_w 8.7).

As for Malaysian territories, the most seismically active zones are Sabah and Sarawak, while Peninsular Malaysia remains the least seismically active. Sabah has several faults that are identified as active, such as Mensaban, N-S trending Perancangan, E-W trending Lahad Datu, Keningau, Danim, Binuang, Tabin and Beluran Faults [42]. Yan [42] has pointed out that the maximum magnitude earthquakes were recorded in Lahad Datu Fault in 1976 (M_w 5.8), and Binuang and Beluran Faults each with M_w 4.3. Nonetheless, in Sarawak, faults that could generate earthquakes identified as active are Tabau and Kelawit Faults with M_w 5.2 in May 2004 and M_w 3.5 in January 2010 respectively. However, in Peninsular Malaysia, there were a series of tremors felt in the Bukit Tinggi area around November 2007 (M_w 2.9) and October 2009 (M_w 3.5). These were assumed to be generated by the Bukit Tinggi Fault, which was considered inactive [42], but could be going through re-activation.

C. SEISMIC HAZARD ANALYSIS TYPES AND METHODS

After unfortunate events, such as earthquakes, it is human nature to demand for appropriate actions to minimize loss of life and property when similar disasters strike again. Even though earthquakes have occurred almost systematically throughout history, it was only with the advances of science that scientists have started to research ways of quantifying hazard posed by earthquakes in their vicinity. The Long Beach earthquake of 1933 in United States was an event that prompted officials to enforce earthquake resistance into the design of school buildings [43]. Since then, SHA methods have significantly evolved. SHA is widely utilized in engineering today to give some certain measurement to the hazard posed by uncertain earthquake sources [44], [45], and is used in design applications to develop earthquake resistant structures and risk assessment/management applications [46]. It is an established topic in the literature, with considerable research conducted on all aspects of ground motion predictions, although it is observed that hazard predictions can still fail or are almost impossible to validate [47].

Up until the 1970s, hazard was estimated using the largest earthquake that occurred around the site plus an increment of 0.5 [48]. Such methodology was problematic, as when the site was located within the tectonic province, earthquake occurrence directly below the site was not even considered due to the assumption of its unlikely nature. This has led to the erroneous practice of negotiating the source location with regulators [48]. There are two notable methods that are widely used throughout industry today: Probabilistic SHA (PSHA) and Deterministic SHA (DSHA).

1) PROBABILISTIC SEISMIC HAZARD ANALYSIS

PSHA is simply a term that is used for all seismic hazard analysis method, which attempts to define either the frequency of events or the frequency of exceedance of some parameters. These are PGA, PGV, SA and combining all the earthquake data for the region using statistical methods [49], [50]. PSHA PSHA has its roots in the methodology proposed by Cornell [44] and improved by McGuire [51] and later improved by the same author McGuire [52] and expanded for the treatment of uncertainties (earthquake location, size, medium of propagation and others) by using expert opinion in the guidelines proposed by [53] and [54].

PSHA is rather complicated, as it uses complex statistical formulations, taking into consideration all the available earthquake data, regardless of magnitude. However, earthquakes with magnitudes of less than 5 are assumed non-damaging and usually ignored to simplify the calculations [15]. The primary output of such exercise is a hazard curve, plotting ground motion parameter (such as PGA or SA) against the annual frequency of exceedance. Equation (3) [44], [51], shows the integral used to compute SHA in probabilistic terms:

$$\lambda_{Y>y} = \sum_{i=1}^{N} V_i \left\{ \int_{r_{\min}}^{r_{\max}} \int_{m_l}^{m_u} p\left[Y > y \,|m, r\,\right] f_{M,R}(m, r) dmdr \right\}_i \tag{3}$$

where

N	total number of the seismic sources;
V_i	mean annual rate of occurrence of earthquakes generated by source i with magnitudes between m_l and m_u;
r_{min}/r_{max}	minimum and maximum source-to-site distances for source i;
m_l/m_u	lower and upper-bound values of magnitude for source i;
$p[Y > y\|m,r]$	conditional probability that an earthquake of magnitude $M = m$ at distance $R = r$ from the site would cause ground motion with parameter $Y > y$;
$f_{M,R}(m,r)$	joint probability density function of magnitude M and distance R

Poisson distribution is central to the earthquake occurrence model in PSHA. Therefore, it assumed that all variables are independent of each other [16], [55]. On the other hand, Chandler et al. [56] state that for relatively rare, moderate to large magnitude earthquakes, the assumption of independent events is reasonable as it is the uniform areal seismicity rate assumption that earthquakes occur uniformly in regions with low to moderate seismicity, so that the uniform seismicity assumption goes in part with Poisson model. Even though some researchers dispute the use of the Poissonian model for earthquake occurrence [57], the use of it greatly simplifies work and results in minor errors [58], [59]. To achieve Poissonian distribution, seismic catalogs are filtered to remove fore- and after-shocks using Gardner and Knopoff's method [60].

As modern PSHA analyses involve huge data sets and various attenuation relationships, it is quite common that logic tree approach will be utilized [17]. Logic tree is a method to combine multiple variations of models and assumptions by assigning to them a certain weightage. When analysis is performed, the computer will automatically calculate the amount of contribution from each model to the final result according to the weightage assigned [61]. SSHAC guidelines specify the procedures to follow when using the logic tree approach [53].

Since the return period and chances of exceedance play a central role in SHA result formulation and presentation, choosing an appropriate return period for design can be quite challenging. Currently, designers choose a life-expectancy, termed exposure period, of a building at 50 years [56], and calculate the hazard parameter that has 2% or 10% chance of being exceeded. A 10% chance of occurrence in 50 years corresponds to 475 years return period, and is chosen for most building designs [62], [63], while a 2% chance of occurrence in 50 years corresponds to 2475 years return period, and is chosen for buildings that are of high importance, like nuclear power stations and dams [64].

Scenario earthquake is desired for design analysis or other seismic risk decisions. Thus, hazard deaggregation procedure is utilized in PSHA. Deaggregation procedure allows the separation and understanding of the contribution of each source to the calculated hazard [50]. Also, it is used to identify those magnitudes, distances and ground motion uncertainty that mostly affect the results [65].

2) DETERMINISTIC SEISMIC HAZARD ANALYSIS

DSHA procedures utilize the available seismicity catalogues, geological and velocity model data and the known seismic source parameters near the investigated site to generate models of ground motion near the site [63], [66]. It is done by choosing a maximum credible earthquake (MCE) and calculating ground shake from it alone. A particular feature of DSHA is that it calculates the ground motion considering a single large magnitude earthquake for each source, the MCE, which in reality will account for all other earthquakes less than MCE. In practice, MCE is estimated from a maximum magnitude supported by geological evidence, which is later added an extra increment of 0.25, 0.5 or approximated up to the nearest quarter magnitude to form the final best-estimate magnitude, the MCE [43], [45]. Such an action is to ensure the needed conservatism for the design of the structures that takes into consideration the uncertainty of the earthquake phenomenon. When there are several sources around the site, the source that causes maximum effect on the site is considered the estimated resultant DSHA [67].

D. GROUND MOTION MODELS

When an earthquake event occurs, the released energy moves through the ground in the form of waves. As the earth crust is composed of various layers of varied media, laid out in various angles and thicknesses, those waves lose energy with the distance traveled, or "attenuate". There are two main types of earthquakes according to source type: interplate and intraplate earthquakes. The interplate earthquakes occur along or parallel to the plate boundaries. This includes thrust earthquakes at subduction zones and strike-slip earthquakes along transform boundaries. Earthquakes located at a distance from the boundaries at the plate interior are called intraplate earthquakes, and typically have more moment release [68]. Most ground motion models, sometimes termed ground motion prediction equations (GMPEs), attenuation equations or relationships, are developed to suit each particular source type, as each source has different attenuation characteristics. Petersen *et al.* [9] summarise the available GMPEs in four groups, such as:

a) interplate crustal earthquakes near plate boundaries;
b) intraplate crustal earthquakes within stable continental regions;
c) intermediate and deep earthquakes within the subducting slab;
d) subduction zone earthquakes on the plate interface. Fig. 3 shows the earthquake sources for subduction zone.

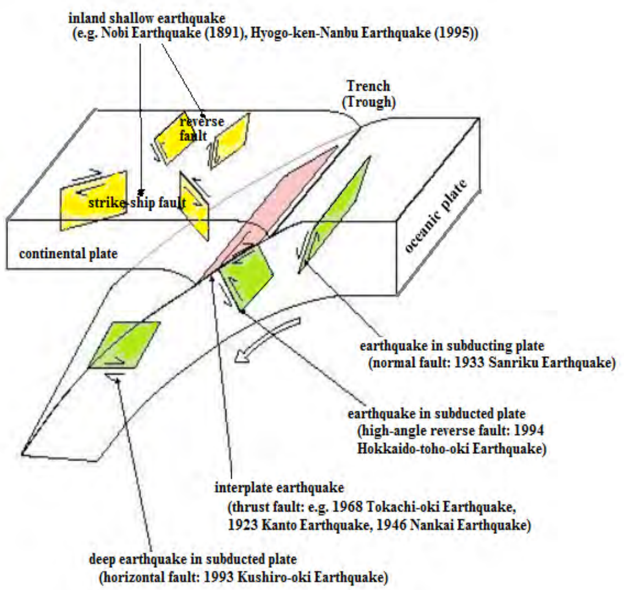

FIGURE 3. Earthquake sources at subduction zones (Source: Japanese Headquarters for Earthquake Research Promotion).

Up until now, there have been many recordings of ground motion all around the world. Most GMPEs have been developed empirically from these data. These relates ground motion recordings to magnitude, depth and distance using regression analyses [37]. Equation (4) [16], describes this relationship.

$$\ln(\mathrm{Y}) = \mathrm{f}(\mathrm{M,R,D}) + \varepsilon\sigma \tag{4}$$

where

Y ground motion parameter (PGA, PGV, MMI, PSA, RSA)
M magnitude
R distance
D depth
ε normalized residual
σ standard deviation

The importance of choosing a correct GMPE is undeniable as very large variations in results can be observed with little change in equation [43]. There is a great degree of variance in all observed data. The recordings of any parameter will vary from earthquake to earthquake, from rupture mechanism to depth information, even for the similar magnitudes [17]. In fact, for the same event, the recordings will vary at stations located at similar distances. Such variance results in the inability of the mean of the developed regression curve to pinpoint all the ground motion data, resulting in some difference between predicted value and actual recording, known as residue [69]. The residues could be attributed to site effects and unknown factors in relationship [43] and is now considered an important part of attenuation equation [17]. In all available equations, an error term ($\varepsilon\sigma$) is added at the end of the regression curve to specify the standard deviation to account for the residue, usually avoiding the truncation below $\varepsilon = 3$ [17].

There are two main ways to model an attenuation equation: 1) to do an empirical regression analysis using real recordings [69], [70] or 2) to use synthetic seismograms method to calculate ground motion and use that data to model an equation [21], [71].

TABLE 1. Example of developed GMPES used for Malaysia.

ATTENUATION MODELS	TARGET REGION
Youngs et al. [19]	Global
Atkinson and Boore [20]	Cascadia
Zhao et al. [72]	Japan
Kanno et al. [73]	Japan
Lin and Lee [74]	Taiwan
Megawati et al. [21]	Singapore

Some regions of the world lack sufficient data or funding to develop a specific relationship for those regions. Therefore, it can be seen that attenuation relationships developed for other regions have been used. Examples of the developed GMPEs, which have been used in replicating Malaysia's ground motion can be seen in Table 1. Also, it has been warned that regionally validated model of attenuation relationship should be utilized, not the imported one [17]. Furthermore, Lam *et al.* [18] shows in his study that a slight mismatch of GMPE to the regional characteristics can lead to SHA estimates that are several orders higher on the log scale than the real recordings, as shown in Fig. 4. In this figure, one can observe a great difference between the model by Megawati *et al.* [41] predicted against the seismic recordings for the 2004 Aceh earthquake and 2005 Nias earthquakes.

Overall, the GMPE relates magnitude, distance and depth to a certain earthquake parameter, like PGA or PGV.

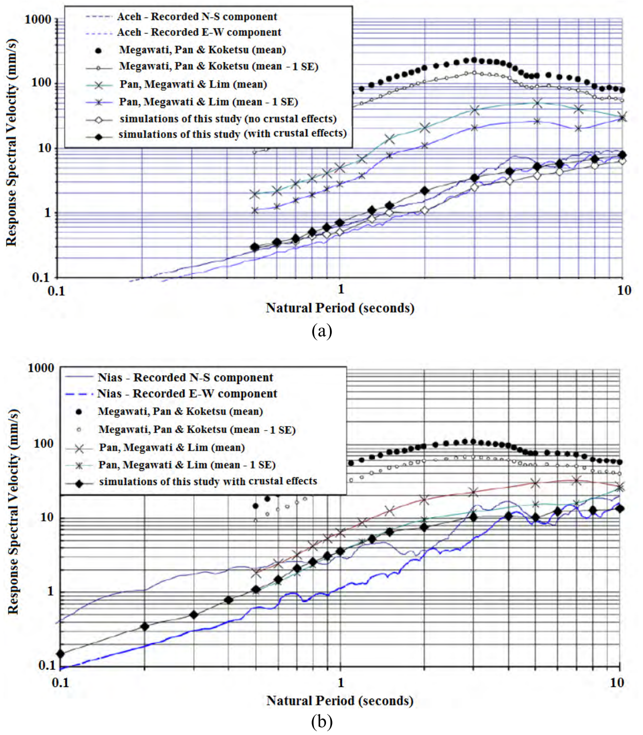

FIGURE 4. Estimates by 3 different models vs. recorded earthquakes [18]. (a) Aceh earthquake scenario (M9.3 at 1200 km). (b) Nias earthquake scenario (M8.6 at 750 km).

There have been numerous GMPEs proposed by researchers. Some of this research has even been conducted for Malaysia [9], [75]–[77]. Despite this, GMPEs from different regions have been utilized in SHAs for Malaysia up until now. Thus, these literatures have shown that there is a need to develop a regional GMPE to be used in further Probabilistic Seismic Hazard Analyses specifically for Malaysia. As such, this work aims to produce a Malaysia-specific GMPE that will cater for the unique conditions of seismic propagation in Malaysian territories.

III. METHODOLOGY

A. DATA GATHERING AND ACQUISITION

As this research attempt is concerned with ground motion, only the earthquakes that cause some shake are of interest. Fortunately, the Malaysian Meteorological Department (MET), has an array of data that records peak ground acceleration (PGA) as felt in various stations throughout Malaysia. However, these data were available only since 2004, for a period of 10 years, totaling at 47 seismic events.

However, upon the acquisition of these data, it was found that each seismic event was recorded at multiple stations located at various distances spread out spatially throughout Peninsular Malaysia, Sabah and Sarawak. This meant that each recording could be considered independent, greatly increasing the size of the data. Overall, there are 457 recordings in the database for this research.

FIGURE 5. Map depicting the locations of MET seismic stations in Malaysia (source: Google Inc.)

FIGURE 6. Map of origins of felt earthquakes in Malaysia by MET.

B. SOURCE CHARACTERIZATION AND GROUPING OF EARTHQUAKES

It was established in the literature review that earthquake attenuation changes with the earthquake source type. That is why there is a need to group earthquakes according to the types of sources, and generate GMPE specific for that type. Fig. 6 shows the map of origins of felt earthquakes in Malaysia provided by MET.

The PGA catalog containing 47 earthquakes provided by MET has only location, depth and magnitude information, as do the other catalogs by NEIC and ISC. The identification of the source type is not straightforward when it comes to subduction zones, as there are shallow subduction interface earthquakes, deep subduction earthquakes and backarc seismicity associated with the Sumatran fault located in the same region. Thus, the establishment of source types and grouping of earthquakes according to the source in Sumatran Subduction Zone had to be done manually.

This was performed in four steps:

1) Extract earthquakes in the study window from NEIC online catalogue. Group those earthquakes in clusters in such a way as to avoid excessive spread-out of earthquakes.

2) Choose an arbitrary point perpendicular to the dipping line of each cluster to calculate distances from each earthquake within the cluster to that arbitrary point. The Distance vs. Depth graph will be an approximate cross-section of the cluster.

3) In the Distance vs. Depth graph, identify the shallow subduction source, deep subduction source and earthquakes due to backarc seismicity.

4) Find the earthquakes of MET PGA catalogue in the graph to classify their source.

First, a study window was set between −4° to 11° Latitude and 96° to 105° Longitude to correctly contain the Sumatran Subduction Zone. The earthquakes in this window were extracted from the NEIC online catalog. This resulted in 975 events occurring from 1973 to 2013 with magnitudes above M_w 5.

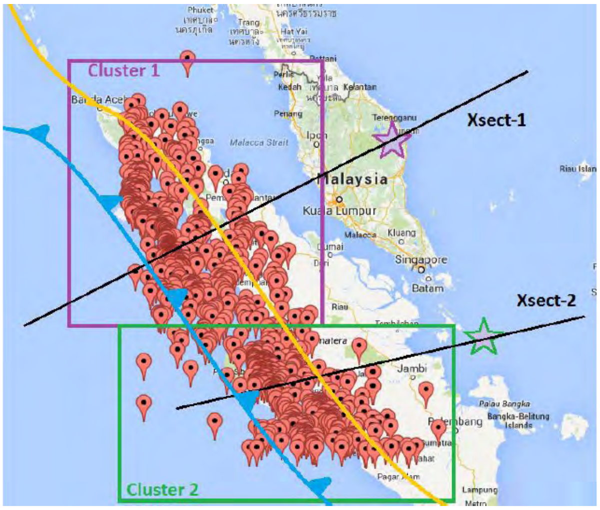

FIGURE 7. Earthquakes in NEIC catalogue grouped into two clusters of earthquakes with appropriate arbitrary points and the line of cross-section. Yellow line depicts Sumatran Strike-Slip fault, blue line depicts Sumatran Subduction.

As the study window is quite spaced-out diagonally, it was deemed fit to divide the earthquakes in the study window into two clusters at 0° Latitude. With the aim of taking a cross-section, an arbitrary point was selected for each cluster perpendicular to the subduction line some long distance away to eliminate the effect of lateral spacing among the earthquakes within the cluster. Fig. 7 shows two clusters of earthquakes, as well as the cross-sections. For cluster 1 (North Sumatra) the point is located at 4° Latitude 103° Longitude, while for cluster 2 (South Sumatra) the point is located at 0° Latitude 105.3° Longitude. Clusters 1 and 2 are separated by the Equator line. The distance from the Sumatran Strike-Slip fault and Sumatran Subduction Zone to the arbitrary points are approximately 500km and 600-700km respectively.

Thereafter, the distances from each earthquake in the NEIC catalogue to the established arbitrary points were calculated and the depth versus distance graphs (Fig. 8 and Fig. 9) were plotted for both clusters. In Fig. 8 and Fig. 9, one can clearly see two tectonic plates in contact, where oceanic plate subducts under continental plate and extends very deep downwards, all this accompanied by earthquakes of various sizes. Three different earthquake sources are visible, as earthquakes are bunched around the source at specific distances. For example, at some 500km away from our arbitrary points, earthquakes that come from the Sumatran Strike slip fault, or backarc seismicity can be seen.

In the next step, Subduction zone earthquakes recorded by MET were mapped, shown in Fig. 10. These earthquakes were identified and located in Fig. 8 and Fig. 9, and that is how the source of each MET PGA catalogue earthquake was established.

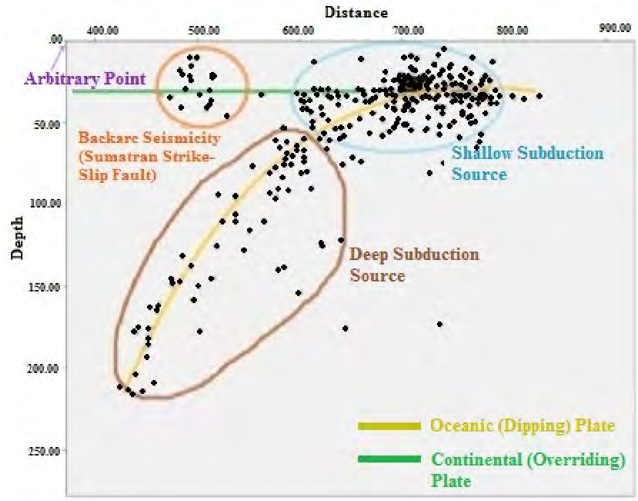

FIGURE 8. Cluster 1 (North Sumatra) earthquakes plot of depth vs. distance.

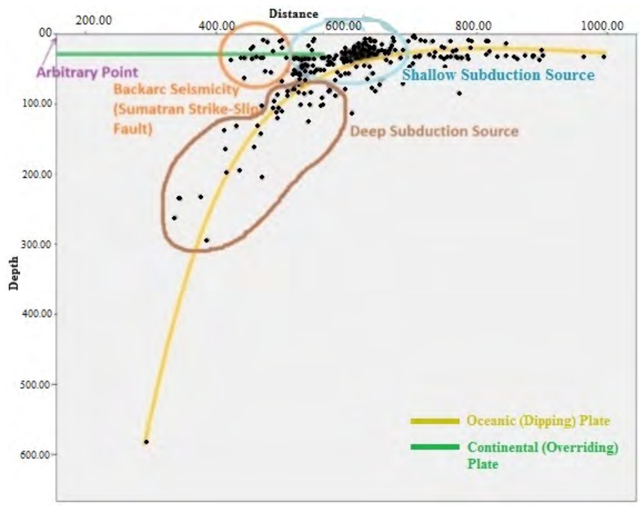

FIGURE 9. Cluster 2 (North Sumatra) earthquakes plot of depth vs. distance.

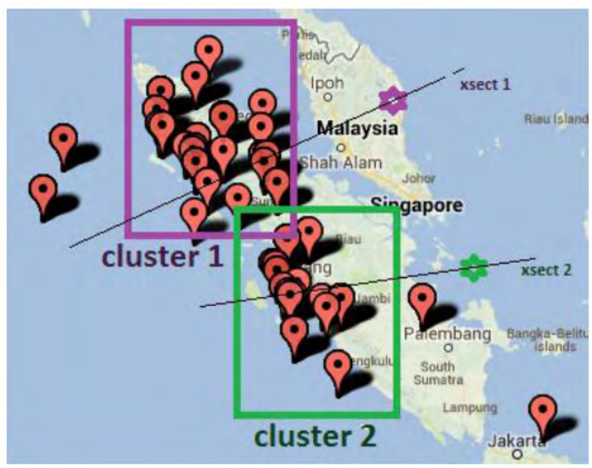

FIGURE 10. Sumatran earthquakes in MET catalogue.

The following bullet-points present a brief analysis of the sources and the data available for their empirical analysis.

- Shallow Sumatran subduction zone interface events (referred as shallow subduction events henceforth) occur at the "interface", or the contacting sides of the two plates, thus they are shallow and could potentially emit great amounts of energy. There are 27 earthquakes felt in Malaysia that are in this group. Shallow subduction earthquakes are very frequent with great variations in energy release, and are located at great distances from Malaysian soils, thus it was decided to ignore earthquakes less than M_w 7 in this research. As such, only 10 earthquakes with 111 recordings were used to represent shallow subduction events;
- Deep subduction earthquakes occur as subducting oceanic plate continue to dip, normally at depths greater than 70km. There are 8 deep earthquakes in the catalogue by MET, of which 6 are located in the Sumatran subduction zone. Again, very low-energy events had to be filtered out from the database; in the case of deep subduction events, it was decided to ignore earthquakes less than M_w 6, resulting in the removal of 1 earthquake. The reason why M_w 7 was not used as the threshold like in the case of shallow subduction earthquakes is that deep subduction events do not release as much energy. Thus, 5 earthquakes with 65 combined recordings were used to model deep subduction earthquakes;
- Continental plate suffers deformations and frequently releases smaller amounts of energy along the Sumatran subduction zone in the Sumatran fault (henceforth referred to as backarc seismicity). 7 earthquakes of this source have been felt in Malaysia, totaling at 82 recordings.
- Two deep earthquakes occurred in Java and Celebes seas, three shallow earthquakes occurred in faults around Sabah region and two great intraplate earthquakes occurred in faults of the Indian oceanic plate. However, more earthquakes are needed to fully capture the characteristics of generation and propagation of seismic waves at these sources, and as a result, these seven earthquakes were also ignored in this study.

C. SELECTION OF THE METHOD FOR GMPE GENERATION

Achieving a statistically significant representative sample size is a main prerequisite for a successful empirical GMPE generation through regression analysis. In this research, it could be said that the data recorded is plausible for empirical method for Sumatran Subduction Zone, because:

- 22 earthquakes (258 recordings) are present. These numbers are enough to establish a pattern in attenuation, as a majority of the earthquakes are closely spaced, and recorded at the same stations;
- 2004 Aceh, 2005 Nias earthquakes and March 2012 earthquakes are among the considered records, together with an array of smaller-sized earthquake recordings, shedding light upon energy attenuation in proportion to the energy released.

In light of these arguments, real recordings will be utilized to generate GMPE empirically through regression analysis for the Sumatran Subduction Zone only, as opposed to the usage of a synthetic seismogram method using the Statistical Package for Social Science (SPSS) software. Other earthquakes from MET database coming from different sources will be ignored in this study, as the sample size is small.

D. VARIABLES AND CORRELATION ANALYSIS

To do a regression analysis, one has to identify the dependent and independent variables, as well as to eliminate variables that lack any observable relationship. In the case of this research, the variables are:

- Moment magnitude
- Body wave magnitude
- Depth
- Distance
- Acceleration in North-South direction
- Acceleration in East-West direction
- Highest of North-South and East-West accelerations
- Diagonal of North-South and East-West accelerations

Out of the listed variables, acceleration has to be chosen as the dependent variable as ground acceleration is a final product of earthquakes, but station-recorded North-South or East-West accelerations vary in size or are sometimes absent. Since only one indicative acceleration is needed, the highest of the values could be taken. However, ground motion does not occur in strict North-South or East-West directions, but happens in random directions. If a particular ground motion occurs in some arbitrary direction, station seismometers will record it by its components in North-South and East-West directions. Thus, taking diagonal North-South and East-West directions will be more appropriate, and is chosen as the dependent variable for this study.

Moment magnitude, body-wave magnitude, depth and distance will automatically become the independent variables. To choose the variable that has more relationship with the dependent variable, a correlation analysis has to be done. A simple correlation analysis is done using a bivariate analysis by Pearson coefficients method. Bivariate analysis involves comparing two groups of variables to determine the empirical relationship between them [78]. The Pearson coefficients method is the most common way of conducting a bivariate analysis, and it measures the linear relationship between two variables. The variables used in this analysis are moment magnitude (M_w), Body-Wave magnitude (mb), epicentral distance, focal depth/distance, and diagonal acceleration.

E. REGRESSION ANALYSIS

Whenever there are variables available, there could be a theoretical reason to relate those variables to each other. A Regression Analysis is a powerful tool to verify the existence of that relationship, as well as to quantify that relationship to a point where we could estimate one variable if the other variable(s) is (are) given [79].

The available data suggests that the linear relationship is not applicable for a regression analysis, thus a non-linear method was used. To carry out a non-linear regression analysis, Statistical Package for Social Science (SPSS) Version 17.0 uses Levenberg-Marquardt algorithm by default, also known as 'damped least-squares method', to fit the curve to the available data [80], [81]. When the parameters are constrained, the default algorithm utilized by SPSS Version 17.0 is Sequential Quadratic Programming algorithm developed by [82] and [83]. For this study, the parameters will not be constrained.

To perform a non-linear regression analysis, functional form for equation has to be assumed for trial-and-error estimation of the true equation. Currently, there are two commonly utilized forms in GMPEs [84]:

i. The shape of the attenuation with distance is independent of magnitude, thus the attenuation relationship takes the form as in (5).

$$\ln Y(M,D,d) = c_1 + c_2 \times M + c_3 \times M^2 + c_4 \times \ln(D + c_5) + c_6 \times d \quad (5)$$

where

Y	parameter to be estimated (PGA)
M	moment magnitude
D	distance
d	depth
c_1-c_7	coefficients

ii. The attenuation with distance is dependent on magnitude, thus functional form has to be taken as in (6):

$$\ln Y(M,D,d) = c_1 + c_2 \times M + c_3 \times M^2 + c_4 \times \ln(D + c_5 \times \exp(c_6 \times M)) + c_7 \times d \quad (6)$$

Using the above-mentioned functional forms, a non-linear regression analysis is conducted using SPSS. Throughout the experimentation with the various functional forms, R-squared value was used as the indicator of the goodness-of-fit of the equation to the available data. The closer the R-squared value to 1, the better the generated regression line will fit the data.

F. COMPARISON WITH AVAILABLE GMPEs AND RECORDED DATA

To verify the accuracy of the results, as well as to prove the point of originality, the following methods were chosen:

- GMPEs that are applicable for subduction events in the literature will be chosen and PGA estimations will be generated for each recording. Estimates of the GMPEs of this study will be generated as well;
- Percentage difference between diagonal acceleration and the estimations by all GMPEs will be calculated: their descriptive statistics will be generated and histograms will be plotted to identify which GMPE fits the data better.
- The accuracy of the prediction of the attenuation mechanism will be tested by choosing three characteristic earthquakes for each source and plotting GMPE estimations on acceleration vs. distance graph.

Thus, the empirical method of GMPE generation was chosen as the methodology for this study as data acquired from MET is sufficient for such a task. GMPEs have been generated for three earthquake types that are shallow subduction earthquakes, deep subduction earthquakes and backarc seismicity. Therefore, the generated GMPEs have been compared with models proposed in the literature, as well as with real ground motion recordings for four cities around Malaysia.

IV. RESULTS AND DISCUSSIONS

This section deals with overall results obtained as per the methodology discussed in the previous section.

A. CORRELATION ANALYSIS

A correlation analysis was conducted using SPSS Version 17.0 involving all variables available for each source as per the methods discussed in the previous section. The results have been presented in form of tables where Pearson correlation represent correlation between variables. The ideal value will be greater than 0.3 but not more than 0.8. The significance of the correlation represented by Sig. (2-tailed) with confidence interval of 0.01 and 0.05 indicating 99% and 95% confidence level. Number of sample used in the analysis is denoted by N.

TABLE 2. Correlation values for shallow subduction sources.

		Magnitude Moment	Magnitude Body	Epicentral Distance	Focal Distance	Depth	Diagonal Accel.
Magnitude Moment	Pearson Correlation	1	.274**	.155	.155	-.365**	.335**
	Sig. (2-tailed)		.004	.104	.105	.000	.000
	N	111	111	111	111	111	111
Magnitude Body	Pearson Correlation	.274**	1	.004	.005	.543**	.413**
	Sig. (2-tailed)	.004		.965	.962	.000	.000
	N	111	111	111	111	111	111
Epicentral Distance	Pearson Correlation	.155	.004	1	1.000**	-.045	-.531**
	Sig. (2-tailed)	.104	.965		.000	.636	.000
	N	111	111	111	111	111	111
Focal Distance	Pearson Correlation	.155	.005	1.000**	1	-.045	-.531**
	Sig. (2-tailed)	.105	.962	.000		.639	.000
	N	111	111	111	111	111	111
Depth	Pearson Correlation	-.365**	.543**	-.045	-.045	1	.067
	Sig. (2-tailed)	.000	.000	.636	.639		.482
	N	111	111	111	111	111	111
Diagonal Accel.	**Pearson Correlation**	**.335****	**.413****	**-.531****	**-.531****	**.067**	**1**
	Sig. (2-tailed)	.000	.000	.000	.000	.482	
	N	111	111	111	111	111	111

**. Correlation is significant at the 0.01 level (2-tailed).

1) SHALLOW SUBDUCTION EARTHQUAKE SOURCES

Table 2 shows the correlations between the variables for shallow subduction events. A few remarks have to be made such as:

- Pearson correlations between diagonal accelerations, moment magnitudes and body-wave magnitudes are shown to be significant, indicated by double asterisks. Since these magnitudes are designed to measure different characteristics of an earthquake, using both of them should shed more light upon patterns that will enrich the generated GMPE;
- Epicentral and focal distances have the exact same correlations with diagonal ground acceleration, the reason

being that the depths at which this group of earthquakes occur are very shallow, making these variables identical at great distances. Thus, only epicentral distance was used for shallow subduction sources;

- Depth has very little correlation with diagonal acceleration, but in the study of earthquakes, where great amounts of unknown variables exist that play their individual roles from generation to ground acceleration, one cannot ignore even the slightest contributor. Depth, in this sense, was also added into the process of GMPE generation.

TABLE 3. Correlation values for backarc sources.

		Magnitude Moment	Magnitude Body	Epicentral Distance	Depth	Focal Distance	Diagonal Accel.
Magnitude Moment	Pearson Correlation	1	.895**	.542**	-.642**	.542**	-.485**
	Sig. (2-tailed)		.000	.000	.000	.000	.000
	N	82	82	82	82	82	82
Magnitude Body	Pearson Correlation	.895**	1	.567**	-.685**	.567**	-.462**
	Sig. (2-tailed)	.000		.000	.000	.000	.000
	N	82	82	82	82	82	82
Epicentral Distance	Pearson Correlation	.542**	.567**	1	-.249*	1.000**	-.470**
	Sig. (2-tailed)	.000	.000		.024	.000	.000
	N	82	82	82	82	82	82
Depth	Pearson Correlation	-.642**	-.685**	-.249*	1	-.247*	.300**
	Sig. (2-tailed)	.000	.000	.024		.025	.006
	N	82	82	82	82	82	82
Focal Distance	Pearson Correlation	.542**	.567**	1.000**	-.247*	1	-.469**
	Sig. (2-tailed)	.000	.000	.000	.025		.000
	N	82	82	82	82	82	82
Diagonal Accel.	Pearson Correlation	-.485**	-.462**	-.470**	.300**	-.469**	1
	Sig. (2-tailed)	.000	.000	.000	.006	.000	
	N	82	82	82	82	82	82

**. Correlation is significant at the 0.01 level (2-tailed).
*. Correlation is significant at the 0.05 level (2-tailed).

2) BACKARC EARTHQUAKE SOURCES

Table 3 shows the results of the correlation analysis done for the database of earthquakes in the backarc zone. Moment magnitude, body-wave magnitude and depth variables were chosen for regression analysis, as significant correlation was observed between these and diagonal acceleration.

As with shallow subduction source, epicentral and focal distances are nearly identical due to shallow depths, thus epicentral distance was chosen for further analyses.

TABLE 4. Correlation values for deep subduction sources.

		Magnitude Moment	Magnitude Body	Epicentral Distance	Focal Distance	Depth	Diagonal Accel.
Magnitude Moment	Pearson Correlation	1	.857**	.496**	.505**	.170	.287*
	Sig. (2-tailed)		.000	.000	.000	.177	.020
	N	65	65	65	65	65	65
Magnitude Body	Pearson Correlation	.857**	1	.394**	.368**	-.221	.314*
	Sig. (2-tailed)	.000		.001	.003	.077	.011
	N	65	65	65	65	65	65
Epicentral Distance	Pearson Correlation	.496**	.394**	1	.995**	.198	-.272*
	Sig. (2-tailed)	.000	.001		.000	.113	.029
	N	65	65	65	65	65	65
Focal Distance	Pearson Correlation	.505**	.368**	.995**	1	.293*	-.287*
	Sig. (2-tailed)	.000	.003	.000		.018	.021
	N	65	65	65	65	65	65
Depth	Pearson Correlation	.170	-.221	.198	.293*	1	-.162
	Sig. (2-tailed)	.177	.077	.113	.018		.196
	N	65	65	65	65	65	65
Diagonal Acceleration	Pearson Correlation	.287*	.314*	-.272*	-.287*	-.162	1
	Sig. (2-tailed)	.020	.011	.029	.021	.196	
	N	65	65	65	65	65	65

**. Correlation is significant at the 0.01 level (2-tailed).
*. Correlation is significant at the 0.05 level (2-tailed).

3) DEEP SUBDUCTION EARTHQUAKE SOURCES

Table 4 shows the results of the correlation analysis done on the database for deep subduction sources. The following remarks have to be made:

- Moment magnitude and body-wave magnitude were utilized in the regression with the same reasoning as in the previous sources;
- The point of difference between deep subduction and other sources is that the deep subduction earthquakes occur at very deep locations (>70km), showing significant differences between epicentral and focal distances. That is why depth variable was used in the regression analysis as in the other sources;
- It can be seen that the correlations are significant at 0.05 level, unlike in the previous sources. This decrease in significance could be attributed to the dynamics of seismic propagation through the various layers in the earth medium, as the earthquake focal point is located very deep in the ground.

B. REGRESSION ANALYSIS

After finalizing the variables through correlation analyses, the next step was concentrated on finding a mathematical relationship between the dependent and independent variables. Non-linear regression equations are found using mathematical transformations of variables. For example, transforming the dependent variable into logarithmic terms will smooth out the data such that the unnecessary large differences will not hinder the regression line generation. The same goes to independent variables, where usage of power transformations (like x^2) will compress the large values of x and spread out the small values of x, thus giving us a better representation of the central tendency.

The method of finding the right non-linear regression equation that fits the data can be summarized in three steps:

1) Transform the dependent variable (Y) using natural logarithm to make Ln(Y)

2) Transform the independent variables (X) using the above-mentioned transformations according to the type of independent variable at hand. The curve estimation function of SPSS Version 17.0 was used to filter out the transformations that were not representative of the dependent-independent variable relationship.

3) Add (7) to represent the assumption that the energy attenuation is dependent on the amount of energy released by the earthquake (the value of mb)

4) Choose and form equations composed of the above-mentioned transformations through trial-and-error, and perform constant estimation for these equations using SPSS non-linear regression analysis function. The equation that has the highest credible R-squared value was chosen.

Upon the establishment of the best-fit relationship between the dependent and independent variables, countless trial-and-error attempts were made to find the best combination of these dependent-independent variable relationships as a functional form utilizing the "Non-Linear Regression" function of SPSS. Functional forms proposed by other researchers were also explored. The functional form similar to one proposed by [19] was chosen for all source types, following the assumption that attenuation of the energy is magnitude dependent. This resulted in the addition of a functional component (7) that catered for the said assumption.

$$Constant \times ln(Distance + e^{(constant \times Magnidute)}) \quad (7)$$

As the fundamental idea of this component deals with the attenuation of energy with distance, body-wave magnitude was chosen to be used for "Magnitude", and the distance that best represents the body-wave propagation path as the "Distance".

The results of these exercises are presented in the following subsections for each source type:

1) SHALLOW SUBDUCTION EARTHQUAKE SOURCES

After trial-and-error attempts, the following non-linear equation was chosen to be used as GMPE for shallow subduction source earthquakes:

$$\ln(\mathrm{PGA}) = C_1 + C_2M_w + C_3M_W^2 + C_4D_e + C_5D_e^3 + C_6\ln(D_e + e^{c_7 mb}) + C_8h + C_9h^3 \quad (8)$$

where

PGA	peak ground acceleration, in g
M_w	moment magnitude, no units
mb	body-wave magnitude, no units
D_e	epicentral distance, in km
h	depth, in km
C_1 to C_9	constants

The constant estimates and Analysis of variance (ANOVA) table for the (8) are shown in Table 5 and Table 6. ANOVA table shows the variation group means through showing the Regression, Residual, Uncorrected and Corrected Total Sum of Squares. These explain the variance between the mean of the actual data and the mean of the generated data by the newly formed regression equation. Coefficient of determination (R^2) is 0.85, showing that the chosen equation with the stated constants fit the data very nicely.

TABLE 5. Constant estimates for equation (8).

C_1	C_2	C_3	C_4	C_5	C_6	C_7	C_8	C_9	σ
-28.778	3.180	-0.147	-0.002	0.8314 $\times 10^{-10}$	0.295	1.026	0.198	-0.4771 $\times 10^{-4}$	0.594

TABLE 6. ANOVA table.

Source	Sum of Squares	df	Mean Squares
Regression	8134.227	9	903.803
Residual	25.473	102	.250
Uncorrected Total	8159.700	111	
Corrected Total	170.230	110	

Dependent variable: In_acc_diag
a. R squared = 1 – Residual Sum of Squares/Corrected Sum of Squares = .850

2) BACKARC EARTHQUAKE SOURCES

Trial-and-error attempts were done similar to shallow subduction earthquake source, and the non-linear equation generated was of the same functional form as in (8). Thus the same equation was used to generate GMPE for Sumatran subduction backarc earthquakes.

TABLE 7. Constant estimates for equation (8).

C_1	C_2	C_3	C_4	C_5	C_6	C_7	C_8	C_9	σ
105.969	-19.923	1.746	0.013	-0.1094 $\times 10^{-8}$	-10.495	-0.048	0.016	0.986 $\times 10^{-6}$	0.656

TABLE 8. ANOVA table.

Source	Sum of Squares	df	Mean Squares
Regression	5491.869	9	610.208
Residual	31.383	73	.430
Uncorrected Total	5523.252	82	
Corrected Total	210.998	81	

Dependent variable: In_acc_diag
a. R squared = 1 – Residual Sum of Squares/Corrected Sum of Squares = .851

The constant estimates and ANOVA table for the backarc earthquakes are shown in Table 7 and Table 8. Again, the coefficient of determination (R2) is 0.851, showing that the chosen equation fits the data quite nicely.

3) DEEP SUBDUCTION EARTHQUAKE SOURCES

Deep subduction earthquakes do not have a similar generation and propagation mechanism as shallow subduction and backarc earthquakes, thus (8) could not be used at it is. Instead, the epicentral distance (D_e) was changed to focal distance (D_f), as earthquakes in deep subduction zone are located very deep, thus their distance traveled will be better represented by D_f. Some modifications were done, and after trial-and-error, Equation (9) was chosen to represent deep subduction earthquakes and used as the GMPE for deep subduction earthquakes of Sumatran subduction zone.

$$\ln(\mathrm{PGA}) = C_1 + C_2M_W^2 + C_3\ln(D_f + e^{c4mb}) + C_5D_f + C_6D_f^3 + C_7D_e^2 + C_8h + C_9h^2 \quad (9)$$

where D_f focal distance, in km.

TABLE 9. Constant estimates for equation (9).

C_1	C_2	C_3	C_4	C_5	C_6	C_7	C_8	C_9	σ
-68.566	0.091	12.858	-3.806	-0.060	-0.6577 $\times 10^{-8}$	0.325 $\times 10^{-4}$	-0.009	-0.4548 $\times 10^{-4}$	0.5

TABLE 10. ANOVA table.

Source	Sum of Squares	df	Mean Squares
Regression	4299.813	9	477.757
Residual	19.777	56	.353
Uncorrected Total	4319.590	65	
Corrected Total	69.600	64	

Dependent variable: In_acc_diag
a. R squared = 1 – Residual Sum of Squares/Corrected Sum of Squares = .716

The constant estimates and ANOVA table for (9) are shown in Table 9 and Table 10. This time, the coefficient of determination is not as high, hinting on more complex attenuation mechanisms of these earthquakes. Still, R2 value of 0.716 could be considered satisfactory.

C. COMPARISON WITH AVAILABLE GMPEs

Finally, as part of the verification attempts, as well as to test the point of originality of this study, the available GMPEs were compared with the current model and the available recordings.

1) GMPEs IN THE LITERATURE

As mentioned before, there are numerous GMPEs in the literature that were used so far to do SHA for Malaysian territories. Out of these GMPEs, Youngs *et al.* [19], Atkinson and Boore [20] and Megawati *et al.* [21] models are the GMPEs that are applicable for subduction zone earthquakes, and they were selected for comparison. Original paper by [19] has specified (10) as the model for attenuation of interface earthquakes for hard rock:

$$\ln(y) = 0.2418 + 1.41 + c_1 + c_2(10 - M)^3 + c_3\ln(r_{rup} + 1.7818e^{0.554M}) + 0.00607H \quad (10)$$

where

y	PGA
M	Moment Magnitude
r_{rup}	closest distance to rupture (km)
H	focal depth

$c_1 = 0$, $c_2 = 0$ and $c_3 = -2.552$

It is timely to note that a modification to Youngs *et al.* [19] model was done according to [9] to make it suitable for long-distance calculations. Thus, the equation takes the form as in (11).

$$\ln(y) = 0.2418 + 1.41 + c_1 + c_2(10 - M)^3 + c_3\ln(r_{rup} + 1.7818e^{0.554M}) + 0.00607H - 0.0038(r_{rup} - 200) \quad (11)$$

Atkinson and Boore [20] have developed their equation for subduction earthquakes shown in (12). NEHRP type B soil was assumed for this study.

$$\log(Y) = c_1 + c_2M + c_3h + c_4\sqrt{(D_{fault}^2 + (0.00724 \times 10^{0.507M})^2)} - 10^{(0.301-0.01M)}\log(\sqrt{(D_{fault}^2 + (0.00724 \times 10^{0.507M})^2)} \quad (12)$$

where

Y	PGA
M	Moment Magnitude
h	focal depth, in km
D_{fault}	focal depth, in km

$c_1 = 2.991$, $c_2 = 0.03525$, $c_3 = 0.00759$, $c_4 = -0.00206$

Megawati *et al.* (2005) used the synthetic seismogram method to generate GMPE, validating the equations through comparisons with the recorded data by Meteorological Service Singapore. The proposed equation is presented in (13).

$$\ln(Y_h) = a_0 + a_1M_w + a_2M_w^2 + a_3\ln(R) + a_4R + a_5H \quad (13)$$

where

Y_h	horizontal PGA
M_w	Moment Magnitude
R	source-to-station distance, in km
H	focal depth, in km
H	focal depth, in km

$a_0 = -7.198$, $a_1 = 2.3691$, $a_2 = -0.013856$, $a_3 = -1$, $a_4 = -0.001548$, $a_5 = -0.08909$.

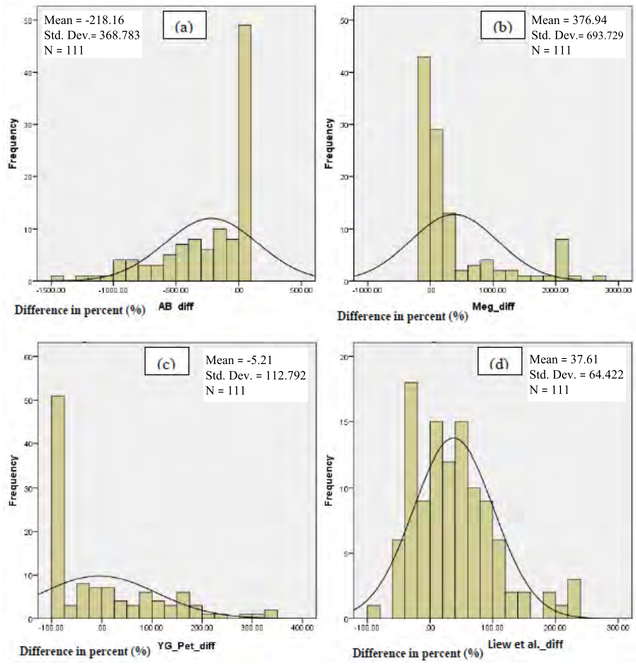

FIGURE 11. Histogram with normal curve for percentage difference for shallow subduction sources.

2) COMPARISON BY PERCENTAGE DIFFERENCE

The percentage differences between the predicted values and the recorded diagonal accelerations were calculated. Fig. 11, Fig. 12 and Fig. 13 show the histograms with normal curves for subduction, backarc and deep subduction earthquake sources respectively. Note that negative numbers indicate underprediction, while positive numbers show overprediction.

Fig. 11(a) shows the percentage difference between the recorded data and the estimates by [20] (denoted as "AB") for subduction source. While a majority of the estimates are quite close to the real recorded values (shown as a spike in the graph), a considerable amount of data severely underpredict the real results, reaching differences as high as 1500%. The opposite is true for the model by [21] (denoted as "Meg") shown in Fig. 11(b), where, despite having a majority of the predictions showing differences in 100-300% range, the model overestimates some predictions by as much as 2500%. Youngs *et al.* [19] model modified by [9] (denoted as "YG-Pet") performs better, shown in Fig. 11(c), having differences in the range of 100-300%, yet its standard deviation and range shows its inferiority to the model proposed by this study (denoted as "Liew *et al.*") in Fig. 11(d). The model proposed by this study generates results that are consistent, with underpredictions within 0-100% range, and overpredictions within 0-250% range. Thus, our model performs best among the models compared.

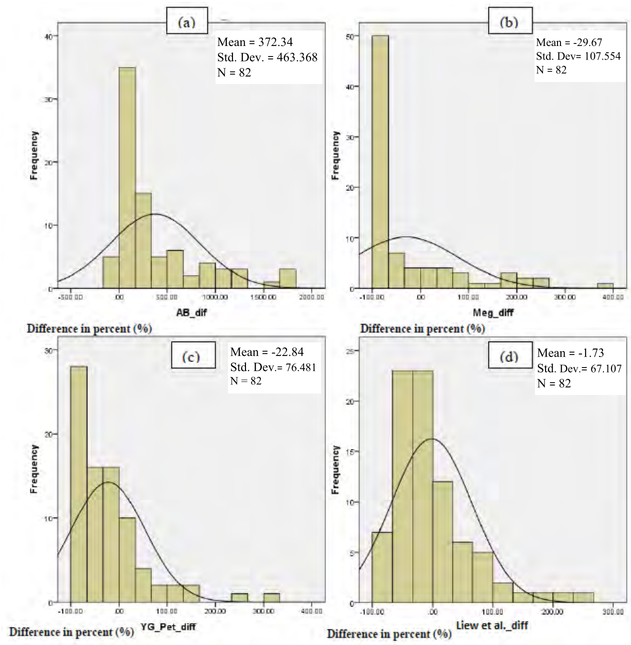

FIGURE 12. Histogram with normal curve for percentage difference for backarc earthquake sources.

Fig. 12(a) shows that for backarc seismicity, the model by [20] fails to properly fit the data. There is a severe overprediction by their model, as differences reach over 1500%. The model by [21] in Fig. 12(b) fairs better, as most of the predictions are within 0-100% range, reaching 300% overprediction at times. Fig. 12(c) shows the percentage difference histogram for the Youngs *et al.* model. The model manages to generate results with a difference of 0-100% than that of real recordings. Similar results are demonstrated by estimates of this study in Fig. 12(d), yet again the model proposed by this study performs better at predicting the ground shake, indicated by a better standard deviation.

Fig. 13(a) and Fig. 13(c) shows that [20] and Youngs [19] models are unable to capture the mechanism of deep subduction earthquakes in the region, predicting estimates reaching 5000% and 8000% differences respectively than that of real recordings. Model by [21] shown in Fig. 13(b) manages to estimate with underprediction in the range of 0% - 100%. Yet the model proposed by this study, shown in Fig. 13(d), fares well with the predictions, with mean, standard deviation and range indicating a much better fit to the data.

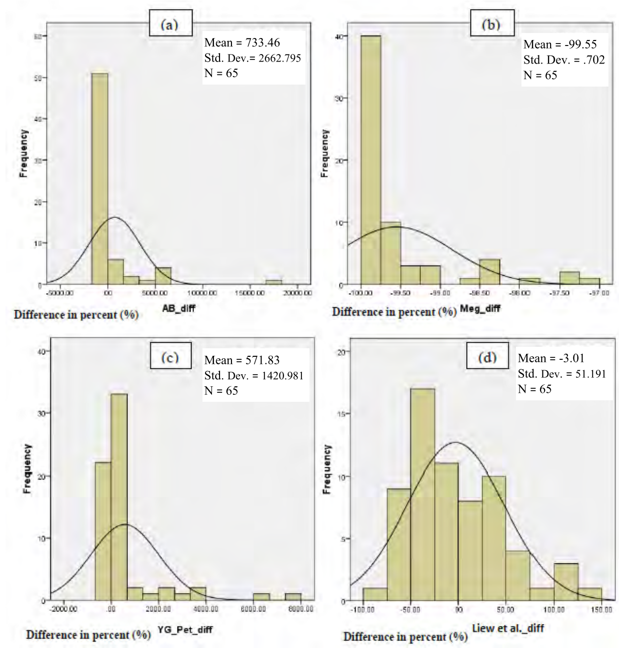

FIGURE 13. Histogram with normal curve for percentage difference for deep subduction sources.

D. EARTHQUAKE SIMULATIONS

The final stage of verification of the models consists of simulations for representative earthquakes for each source. Three earthquake events were chosen: 28 March 2005 earthquake of M_W 8.6 was chosen for shallow subduction earthquake source (Fig. 14), 1 October 2009 earthquake of M_W 6.6 was chosen for backarc earthquake source (Fig. 15) and 30 September 2009 earthquake of M_W 7.6 was chosen for deep subduction earthquake source (Fig. 16). The newly developed GMPEs were compared with developed GMPEs and recorded data by MET. Labelling was used in this study and the details are presented in Table 11.

TABLE 11. Results labelling.

Item/GMPE model	Labeled
Diagonal Acceleration	Diagonal_Acc
Proposed GMPE	Liew et al.
Atkinson and Boore	AB
Megawati et al.	MEG
Petersen et al.	YG_Pet

Fig. 14 reveals that AB and YG_Pet do not accurately represent the attenuation mechanism of shallow subduction earthquakes of the Sumatran Subduction Zone. Their estimates are both overpredicting/underpredicting the ground motion with huge errors, and the steep trendline is unable to properly convey the attenuation. The model by MEG overestimates the ground motion nearly ten times at 500-700km range, the differences keep reducing with the increment in distance. The model proposed by this study (Liew *et al.*) succeeds at representing the attenuation

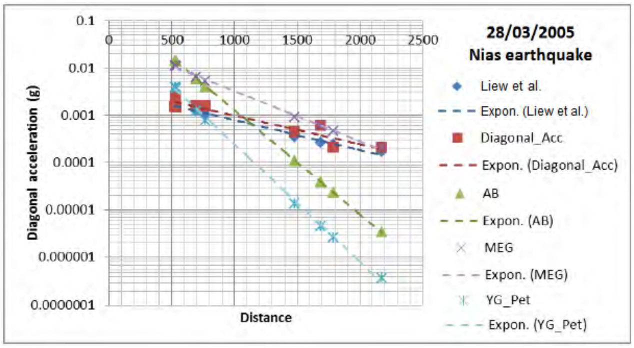

FIGURE 14. 28/03/2005 earthquake simulations along with recorded data.

mechanisms of seismic waves generated by shallow subduction source at both short and long distances. The estimates are closer to the station-recorded values and the mechanism of attenuation with distance is properly captured.

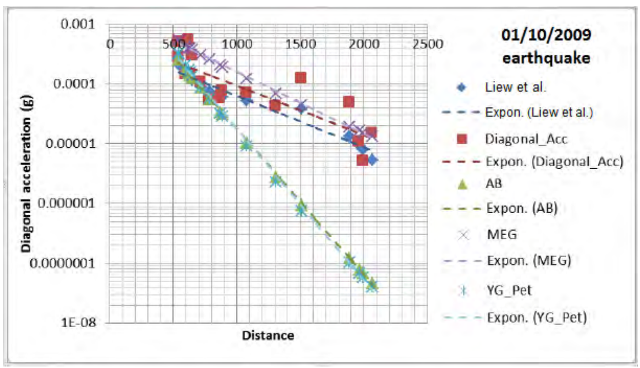

FIGURE 15. 01/10/2009 earthquake simulations along with recorded data.

Fig. 15 shows that models by AB and YG_Pet are again unsuitable for estimating ground motions for backarc earthquake sources in the Sumatran fault for the same reasons as for shallow subduction sources. The models fail to show the accurate attenuation with distance, as well as to deliver results close to station-recorded data. MEG model fairs better than the previous two models, as it is able to capture the attenuation mechanism of the wave more accurately, as well as generate acceptable estimates at 500km range. Yet the overestimation problem starts with increase in distance. The model proposed by this study, on the other hand, manages to follow the same trendline as the station-recorded data, meaning that the model is able to represent the attenuation properly, though slightly underestimating the groundshake. Despite this, the model fits the recorded data better than all other models.

When it comes to deep subduction earthquakes, models by AB, YG_Pet and MEG fail to capture the attenuation mechanism of seismic waves by generating estimates with trendlines completely different to that of the station-recorded data, as shown in Fig. 16. The model proposed by this study

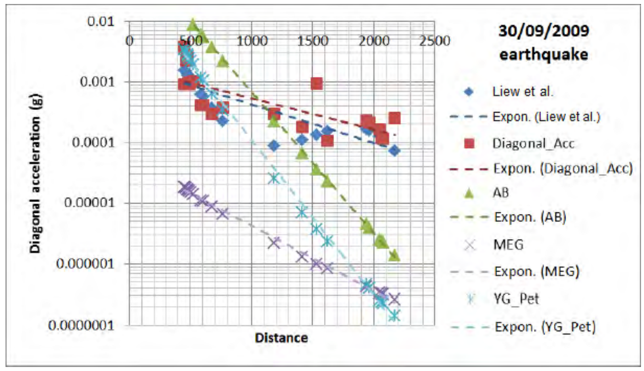

FIGURE 16. 30/09/2009 earthquake simulations along with recorded data.

does well in predicting results that are close to the recorded values and follow the same trendline.

Thus, three GMPEs were generated for shallow subduction, backarc and deep subduction earthquake sources. These GMPEs were compared to GMPEs proposed by Youngs *et al.* [19] modified by Petersen et al. [9], Atkinson and Boore [20] and Megawati [21]. It was found that the generated GMPEs are far superior to the ones available in the literature.

V. CONCLUSIONS

Due to rapid industrialization and development, organizations within Malaysia now have started to pay attention to the protection of assets against possible earthquakes, and to somehow measure the hazard posed by them. From previous studies, the SHA method and GMPE are the two factors which contribute to the error of SHA. While it was shown that the SHA method is highly disputable and currently in the stage of further development, the choice of the method would not have had as much impact on the result as the choice of the GMPE. Thus, this study has attempted to develop GMPE for Malaysia due to the subduction zone earthquakes in the Sumatra region.

A framework for seismic source classification has been produced and three types of earthquakes according to source type known as shallow subduction, backarc and deep subduction have been identified. Then, correlation and non-linear regression analyses were adopted in developing GMPEs for Malaysia based on earthquake source type. Table 12 shows all three GMPEs with the constant estimates.

TABLE 12. GMPEs applicable for malaysian territories due to varied sources.

Shallow subduction	$\ln(PGA) = C_1 + C_2M_w + C_3M^2_W + C_4D_e + C_5D^3_e + C_6 \ln(D_e + e^{c_7mb}) + C_8h + C_9h^3$									
	C_1	C_2	C_3	C_4	C_5	C_6	C_7	C_8	C_9	σ
	-28.778	3.180	-0.147	-0.002	0.8314×10^{-10}	0.295	1.026	0.198	-0.4771×10^{-4}	0.594
Backarc seismicity	Same as shallow subduction GMPE									
	C_1	C_2	C_3	C_4	C_5	C_6	C_7	C_8	C_9	σ
	105.969	-19.923	1.746	0.013	-0.1094×10^{-8}	-10.495	-0.048	0.016	0.986×10^{-6}	0.656
Deep subduction	$\ln(PGA) = C_1 + C_2M^2_W + C_3\ln(D_f + e^{c_4mb}) + C_5D_f + C_6D^3_f + C_7D^2_e + C_8h + C_9h^2$									
	C_1	C_2	C_3	C_4	C_5	C_6	C_7	C_8	C_9	σ
	-68.566	0.091	12.858	-3.806	-0.060	-0.6577×10^{-8}	0.325×10^{-4}	-0.009	-0.4548×10^{-4}	0.5

where

PGA	peak ground acceleration, in g
M_w	moment magnitude, no units
mb	body-wave magnitude, no units
D_e	epicentral distance, in km
D_f	focal distance, in km
h	depth, in km
C_1-C_9	coefficients, no units
σ	standard deviation, no units

In summary, the newly developed GMPE models have been validated: comparisons were made between developed GMPEs and recorded data and three GMPEs from the literature. When compared to the equations proposed by Youngs *et al.* [19] (later modified by Petersen *et al.* [9]), Atkinson and Boore [20] and Megawati *et al.* [21], it was found that the newly generated GMPEs are superior in predicting the ground motions on Malaysian soils. Thus, the three GMPEs generated for Malaysian territories generate the best estimations out of the available equations, and should be used for the Sumatran subduction zone in further SHA studies for Malaysia.

REFERENCES

[1] K. A. Rahim and A. Liwan, "Oil and gas trends and implications in Malaysia," *Energy Policy*, vol. 50, pp. 262–271, Nov. 2012.

[2] T. H. Oh, S. Y. Pang, and S. C. Chua, "Energy policy and alternative energy in Malaysia: Issues and challenges for sustainable growth," *Renew. Sustain. Energy Rev.*, vol. 14, no. 4, pp. 1241–1252, 2010.

[3] (Nov. 21, 2016). *Energy Information Administration*. [Online]. Available: http://www.eia.doe.gov

[4] A. Aulov and M. S. Liew, "Seismic hazard analysis (SHA) considerations for South China Sea territories of Malaysia," presented at the 7th Int. Conf. Geol. Seismol. (GES), vol. 13. Jul. 2013, pp. 173–178. [Online]. Available: http://www.wseas.us/e-library/conferences/2013/Rhodes/ENVIR/ENVIR-30.pdf

[5] *Design of Fixed Offshore Structures (Design and Engineering)*, PETRONAS Technical Standard 34.19.10.30, 2010

[6] M. Z. Ramli and A. Adnan, "Earthquake engineering education plan for low intensity earthquake region," in *Proc. Conf. Eng. Edu. (CEE)*, 2004, pp. 14–15.

[7] N. Musa, "Aceh quake rattles Malaysia," New Straits Times, Malaysia, Tech. Rep. m/s :1, Apr. 2012.

[8] K. McCue, "Seismic hazard mapping in Australia, the Southwest Pacific and Southeast Asia," *Ann. Geophys.*, vol. 42, no. 6, pp. 1191–1198, Dec. 1999.

[9] M. D. Petersen *et al.*, "Probabilistic seismic hazard analysis for Sumatra, Indonesia and across the Southern Malaysian Peninsula," *Tectonophysics*, vol. 390, nos. 1–4, pp. 141–158, 2004.

[10] *Petroleum and Natural Gas Industries—Specific Requirements for Offshore Structures—Part 2: Seismic Design Procedures and Criteria*, International Standard ISO 19901-2, 2004.

[11] P. L.-F. Liu, X. Wang, and A. J. Salisbury, "Tsunami hazard and early warning system in South China Sea," *J. Asian Earth Sci.*, vol. 36, no. 1, pp. 2–12, 2009.

[12] L. Li, A. D. Switzer, C.-H. Chan, Y. Wang, R. Weiss, and Q. Qiu, "How heterogeneous coseismic slip affects regional probabilistic tsunami hazard assessment: A case study in the South China Sea," *J. Geophys. Res., Solid Earth*, vol. 121, no. 8, pp. 6250–6272, 2016.

[13] A. Adnan, A. Marto, and M. Irsyam, "Seismic hazard assessment for peninsular Malaysia using Gumbel distribution method," *J. Teknol.*, vol. 42, no. 1, pp. 57–73, 2012.

[14] M. D. Petersen *et al.*, "New USGS Southeast Asia seismic hazard maps," in *Proc. 14th World Conf. Earthquake Eng.*, 2008, pp. 12–17.

[15] J. W. Pappin, P. H. I. Yim, and C. H. R. Koo, "An approach for seismic design in Malaysia following the principles of Eurocode 8," Jurutera, IEM, Malaysia, Tech. Rep., BIL.2011 No.10, Oct. 2011.

[16] Z. Wang, "Seismic hazard assessment: Issues and alternatives," *Pure Appl. Geophys.*, vol. 168, nos. 1–2, pp. 11–25, 2011.

[17] J. J. Bommer and N. A. Abrahamson, "Why do modern probabilistic seismic-hazard analyses often lead to increased hazard estimates?" *Bull. Seismol. Soc. Amer.*, vol. 96, no. 6, pp. 1967–1977, 2006.

[18] N. T. K. Lam, T. Balendra, J. L. Wilson, and S. Venkatesan, "Seismic load estimates of distant subduction earthquakes affecting Singapore," *Eng. Struct.*, vol. 31, no. 5, pp. 1230–1240, 2009.

[19] R. R. Youngs, S.-J. Chiou, W. J. Silva, and J. R. Humphrey, "Strong ground motion attenuation relationships for subduction zone earthquakes," *Seismol. Res. Lett.*, vol. 68, no. 1, pp. 58–73, 1997.

[20] G. M. Atkinson and D. M. Boore, "Empirical ground–motion relations for subduction–zone earthquakes and their application to Cascadia and other regions," *Bull. Seismol. Soc. Amer.*, vol. 93, no. 4, pp. 1703–1729, 2003.

[21] K. Megawati, T.-C. Pan, and K. Koketsu, "Response spectral attenuation relationships for Sumatran-subduction earthquakes and the seismic hazard implications to Singapore and Kuala Lumpur," *Soil Dyn. Earthquake Eng.*, vol. 25, no. 1, pp. 11–25, 2005.

[22] USGS. (Oct. 22, 2014). *Earthquake Facts and Statistics*. [Online]. Available: http://earthquake.usgs.gov/earthquakes/eqarchives/year/eqstats.php

[23] H. Spall, "Earthquakes and plate tectonics," *Earthquake Inf. Bull.*, vol. 9, no. 6, pp. 14–17, 1977.

[24] Y. Behr, J. Clinton, P. Kästli, C. Cauzzi, R. Racine, and M.-A. Meier, "Restricted access anatomy of an earthquake early warning (EEW) alert: Predicting time delays for an end-to-end EEW system," *Seismol. Res. Lett.*, vol. 86, no. 3, pp. 830–840, 2015.

[25] T. Kusky, and T. M. Kusky, *Earthquakes: Plate Tectonics and Earthquake Hazards*. New York, NY, USA: Infobase Publishing, 2008.

[26] J. Chiang, "Design for seismic action—A far field effect in Malaysia experience," presented at the 3rd ACF Int. Conf. ACF/VCA, Ho Chi Minh, Vietnam, Nov. 2008.

[27] T. Balendra and Z. Li, "Seismic hazard of Singapore and Malaysia," *Electron. J. Struct. Eng.*, no. 1, pp. 57–63, 2008.

[28] P. E. Atimtay and R. Kanit, "Learning seismic design from the earthquake itself," *Pract. Periodical Struct. Des. Construct.*, vol. 11, no. 3, pp. 149–160, 2006.

[29] J. Sun and T.-C. Pan, "Seismic characteristics of Sumatra and its relevance to Peninsular Malaysia and Singapore," *J. Southeast Asian Earth Sci.*, vol. 12, nos. 1–2, pp. 105–111, 1995.

[30] A. Marto, A. Adnan, and M. Irsyam, "Microzonation maps for Kuala Lumpur and Putrajaya," *Malaysian J. Civil Eng.*, vol. 23, no. 1, pp. 63–85, 2011.

[31] W. L. Ellsworth, "Earthquake history, 1769–1989," in *The San Andreas Fault System, California*, R. E. Wallace, Eds. Washington, DC, USA: USG Printing Office, 1990, pp. 153–185.

[32] C. F. Richter, "An instrumental earthquake magnitude scale," *Bull. Seismol. Soc. Amer.*, vol. 25, no. 1, pp. 1–32, 1935.

[33] J. P. McCalpin and A. R. Nelson, "Introduction to paleoseismology," in *International Geophysics*, P. M. James, Ed. San Diego, CA, USA: Academic, 1996, ch. 1, pp. 1–32.

[34] H. Kanamori, "Magnitude scale and quantification of earthquakes," *Tectonophysics*, vol. 93, nos. 3–4, pp. 185–199, 1983.

[35] E. M. Scordilis, "Empirical global relations converting M_S and m_b to moment magnitude," *J. Seismol.*, vol. 10, no. 2, pp. 225–236, 2006.

[36] D. E. Alexander, *Natural Disasters*. Gower Street, U.K.:Springer, 1993.

[37] R. Ulusay, E. Tuncay, H. Sonmez, and C. Gokceoglu, "An attenuation relationship based on Turkish strong motion data and iso-acceleration map of Turkey," *Eng. Geol.*, vol. 74, nos. 3–4, pp. 265–291, 2004.

[38] H. Kanamori, "The energy release in great earthquakes," *J. Geophys. Res.*, vol. 82, no. 20, pp. 2981–2987, 1977.

[39] T. C. Hanks, "b values and $\omega^{-\gamma}$ seismic source models: Implications for tectonic stress variations along active crustal fault zones and the estimation of high-frequency strong ground motion," *J. Geophys. Res., Solid Earth*, vol. 84, no. B5, pp. 2235–2242, 1979.

[40] T. Balendra, N. T. K. Lam, J. L. Wilson, and K. H. Kong, "Analysis of long-distance earthquake tremors and base shear demand for buildings in Singapore," *Eng. Struct.*, vol. 24, no. 1, pp. 99–108, 2002.

[41] K. Megawati, T.-C. Pan, and K. Koketsu, "Response spectral attenuation relationships for Singapore and the Malay Peninsula due to distant Sumatran-fault earthquakes," *Earthquake Eng. Struct. Dyn.*, vol. 32, no. 14, pp. 2241–2265, 2003.

[42] A. S. W. Yan, "Earthquake-generating faults in Malaysia," Malaysian Meteorol. Dept., PJ, Selangor, Malaysia, Tech. Rep. NaTSET-2010, 2010.

[43] L. Mualchin, ''Seismic hazard analysis for critical infrastructures in California,'' *Eng. Geol.*, vol. 79, nos. 3–4, pp. 177–184, 2005.
[44] C. A. Cornell, ''Engineering seismic risk analysis,'' *Bull. Seismol. Soc. Amer.*, vol. 58, no. 5, pp. 1583–1606, 1968.
[45] J.-P. Wang, D. Huang, and Z. Yang, ''Deterministic seismic hazard map for Taiwan developed using an in-house Excel-based program,'' *Comput. Geosci.*, vol. 48, pp. 111–116, Nov. 2012.
[46] J. Klügel and L. Mualchin, ''Earthquake engineering needs and seismic hazard assessment,'' in *Earthquake Resistant Engineering Structures: IX*, vol. 132. Ashurst, U.K.: WIT Press, 2013, pp. 47–67
[47] S. Stein, R. J. Geller, and M. Liu, ''Why earthquake hazard maps often fail and what to do about it,'' *Tectonophysics*, vols. 562–563, pp. 1–25, Aug. 2012, doi: 10.1016/j.tecto.2012.06.047.
[48] J. J. Bommer, ''Uncertainty about the uncertainty in seismic hazard analysis,'' *Eng. Geol.*, vol. 70, nos. 1–2, pp. 165–168, 2003.
[49] J.-U. Klügel, ''Seismic hazard analysis—Quo vadis?'' *Earth-Sci. Rev.*, vol. 88, nos. 1–2, pp. 1–32, 2008.
[50] B. Pace, P. Boncio, F. Brozzetti, G. Lavecchia, and F. Visini, ''From regional seismic hazard to 'scenario earthquakes' for seismic microzoning: A new methodological tool for the Celano Project,'' *Soil Dyn. Earthquake Eng.*, vol. 28, nos. 10–11, pp. 866–874, 2008.
[51] R. K. McGuire, ''FORTRAN computer program for seismic risk analysis,'' U.S. Geol. Survey, Reston, VA, USA, Tech. Rep. 2331-1258, 1976.
[52] R. K. McGuire, ''Probabilistic seismic hazard analysis and design earthquakes: Closing the loop,'' *Bull. Seismol. Soc. Amer.*, vol. 85, no. 5, pp. 1275–1284, 1995.
[53] R. J. Budnitz, G. Apostolakis, and D. M. Boore, ''Recommendations for probabilistic seismic hazard analysis: Guidance on uncertainty and use of experts,'' Nucl. Regulatory Commission, Washington, DC, USA, Tech. Rep. NUREG/CR–6372-VOL.2, 1997.
[54] J.-U. Klügel, L. Mualchin, and G. F. Panza, ''A scenario-based procedure for seismic risk analysis,'' *Eng. Geol.*, vol. 88, nos. 1–2, pp. 1–22, 2006.
[55] A. D. Akkaya and M. S. Yücemen, ''Stochastic modeling of earthquake occurrences and estimation of seismic hazard: A random field approach,'' *Probab. Eng. Mech.*, vol. 17, no. 1, pp. 1–13, 2002.
[56] A. M. Chandler, L. S. Chan, and N. T. K. Lam, ''Deterministic seismic hazard parameters and engineering risk implications for the Hong Kong region,'' *J. Asian Earth Sci.*, vol. 20, no. 1, pp. 59–72, 2001.
[57] E. L. Krinitzsky, ''Epistematic and aleatory uncertainty: A new shtick for probabilistic seismic hazard analysis,'' *Eng. Geol.*, vol. 66, no. 1, pp. 157–159, 2002.
[58] C. A. Cornell and S. R. Winterstein, ''Temporal and magnitude dependence in earthquake recurrence models,'' *Bull. Seismol. Soc. Amer.*, vol. 78, no. 4, pp. 1522–1537, 1988.
[59] R. M. W. Musson *et al.*, ''Evaluating hazard results for Switzerland and how not to do it: A discussion of 'problems in the application of the SSHAC probability method for assessing earthquake hazards at Swiss nuclear power plants' by J-U Klügel,'' *Eng. Geol.*, vol. 82, no. 1, pp. 43–55, 2005.
[60] J. K. Gardner and L. Knopoff, ''Is the sequence of earthquakes in Southern California, with aftershocks removed, Poissonian?'' *Bull. Seismol. Soc. Amer.*, vol. 64, no. 5, pp. 1363–1367, 1974.
[61] A. Frankel, ''Comment on 'Why earthquake hazard maps often fail and what to do about it' by S. Stein, R. Geller, and M. Liu,'' *Tectonophysics*, vol. 592, pp. 200–206, 2013. [Online]. Available: https://doi.org/10.1016/j.tecto.2012.11.032
[62] *1997 Uniform Housing Code*, ICBO, Whittier, CA, USA, 1997.
[63] L. Moratto, B. Orlecka-Sikora, G. Costa, P. Suhadolc, C. Papaioannou, and C. B. Papazachos, ''A deterministic seismic hazard analysis for shallow earthquakes in Greece,'' *Tectonophysics*, vol. 442, nos. 1–4, pp. 66–82, 2007.
[64] *International Building Code*, International Code Council Inc., Country Club Hills, IL, USA, 2000.
[65] R. Romeo and A. Prestininzi, ''Probabilistic versus deterministic seismic hazard analysis: An integrated approach for siting problems,'' *Soil Dyn. Earthquake Eng.*, vol. 20, nos. 1–4, pp. 75–84, 2000.
[66] H. Castaños and C. Lomnitz, ''PSHA: Is it science?'' *Eng. Geol.*, vol. 66, nos. 3–4, pp. 315–317, 2002.
[67] S. L. Kramer, *Geotechnical Earthquake Engineering*. NJ, USA: Prentice-Hall, 1996.
[68] T. Lay and T. C. Wallace, *Modern Global Seismology*. San Francisco, CA, USA: Academic, 1995.
[69] A. Mebarki, ''A comparative study of different PGA attenuation and error models: Case of 1999 Chi–Chi earthquake,'' *Tectonophysics*, vol. 466, nos. 3–4, pp. 300–306, 2009.
[70] L. M. Nguyen *et al.*, ''The first peak ground motion attenuation relationships for North of Vietnam,'' *J. Asian Earth Sci.*, vol. 43, no. 1, pp. 241–253, 2012.
[71] M. Tuluka, ''An estimate of the attenuation relationship for strong ground motion in the Kivu Province, Western Rift Valley of Africa,'' *Phys. Earth Planetary Interiors*, vol. 162, nos. 1–2, pp. 13–21, 2007.
[72] J. X. Zhao *et al.*, ''Attenuation relations of strong ground motion in Japan using site classification based on predominant period,'' *Bull. Seismol. Soc. Amer.*, vol. 96, no. 3, pp. 898–913, 2006.
[73] T. Kanno, A. Narita, N. Morikawa, H. Fujiwara, and Y. Fukushima, ''A new attenuation relation for strong ground motion in Japan based on recorded data,'' *Bull. Seismol. Soc. Amer.*, vol. 96, no. 3, pp. 879–897, 2006.
[74] P.-S. Lin and C.-T. Lee, ''Ground-motion attenuation relationships for subduction–zone earthquakes in northeastern taiwan,'' *Bull. Seismol. Soc. Amer.*, vol. 98, no. 1, pp. 220–240, Feb. 2008.
[75] A. Adnan and M. Suhatril, ''Derivation of attenuation equations for distant earthquake suitable for Malaysia,'' Faculty Civil Eng., Univ. Technol. Malaysia, Johor, Malaysia, Tech. Rep. VOT78266 (UTM RESEARCH MANAGEMENT CENTRE), 2009.
[76] A. B. Nabilah and T. Balendra, ''Seismic hazard analysis for Kuala Lumpur, Malaysia,'' *J. Earthquake Eng.*, vol. 16, no. 7, pp. 1076–1094, 2012.
[77] R. M. Noor, S. W. Ahmad, A. Adnan, and R. Nazir, ''Attenuation function relationship of subduction mechanism and far field earthquake,'' *J. Eng. Appl. Sci.*, vol. 11, no. 4, pp. 2597–2601, Feb. 2016.
[78] E. Babbie, *The Practice of Social Research*, 13th ed. Belmont, CA, USA: Wadsworth, 2013.
[79] R. H. Carver, and J. G. Nash, *Doing Data Analysis With SPSS Version 18.0*. Boston, MA, USA: Cengage Learning, 2011.
[80] K. Levenberg, ''A method for the solution of certain non-linear problems in least squares,'' *Quart. J. Appl. Math.*, vol. 2, no. 2, pp. 164–168, Jul. 1944.
[81] D. W. Marquardt, ''An algorithm for least-squares estimation of nonlinear parameters,'' *J. Soc. Ind. Appl. Math.*, vol. 11, no. 2, pp. 431–441, 1963.
[82] P. T. Boggs and J. W. Tolle, ''Sequential quadratic programming,'' *Acta Numer.*, vol. 4, pp. 1–51, Jan. 1995.
[83] P. T. Boggs and J. W. Tolle, ''Sequential quadratic programming for large-scale nonlinear optimization,'' *J. Comput. Appl. Math.*, vol. 124, nos. 1–2, pp. 123–137, 2000.
[84] Y. Bozorgnia and V. V. Bertero, *Earthquake Engineering: From Engineering Seismology to Performance-Based Engineering*. Boca Raton, FL, USA: CRC Press, 2004.

M. S. LIEW received the B.S.C.E. and Ph.D. degrees from Texas, USA, in 1983 and 1988, respectively. Having been practicing in the offshore industry for 23 years, he is currently the Head of the Offshore Engineering Center and the Deputy Vice Chancellor of Research and Innovation, Universiti Teknologi PETRONAS, Malaysia, where he is also a Professor with the Department of Civil and Environmental Engineering. His focus is on MetOcean, the design of offshore facilities, and on the dynamic aspects of offshore facilities.

He is currently supporting several business units of PETRONAS Carigali, and other oil and gas outfits. As a strong advocate in research with industrial applications, he has innovated several technological advancements in the areas of digital processing in monitoring offshore facilities for its integrity and reliability.

KAMALUDDEEN USMAN DANYARO received the bachelor's degree in mathematics from Bayero University, Kano, Nigeria, the master's degree in business information technology from Northumbria University, Newcastle, U.K., and the Ph.D. degree from Universiti Teknologi PETRONAS, Malaysia. He is currently a Post-Doctoral Researcher and an Integration Engineer with the Offshore Engineering Center, Universiti Teknologi PETRONAS. His current research area is big data management in the oil and gas sector. He is a reviewer in many conferences and journals.

MAZLINA MOHAMAD received the bachelor's degree in civil engineering and the M.Sc. degree in civil engineering (structures) from Universiti Teknologi MARA. She is currently a Lecturer with Universiti Teknologi MARA and a Ph.D. Fellow with Universiti Teknologi PETRONAS.

LIM EU SHAWN received the B.Sc. degree (Hons) in civil engineering from Universiti Teknologi PETRONAS (UTP), Malaysia, with a focus on offshore engineering with particular emphasis on MetOcean, offshore design and asset integrity. He is currently pursuing the Ph.D. degree with UTP, providing active support for research and consultancy works of the Offshore Engineering Centre. He actively involves with various major oil and gas corporations on research and consultancy works, such as PETRONAS, to identify optimizations in their design and operations. He is a C.Eng.

He has involved in training programs via MSSA and MISC Bhd. He represents MSSA in the development of national offshore structures code MS ISO 19901/2. He also involves in active competency building in the offshore engineering industry. He is a member of the Energy Institute. He is also an Accredited Trainer recognized by the Malaysian Human Resource Development Fund.

AZIZ AULOV received the M.Sc. degree in civil engineering from Universiti Teknologi PETRONAS. He is currently a Structural Engineer/Manager who helps solve design/management issues in multinational projects. He is also with Airport Consulting Partners GmbH Beratende Ingenieure, Schwabstraße, Germany.